

# Performance evaluation of 4-quadrature amplitude modulation over orthogonal frequency division multiplexing system in different fading channels scenarios

Hasan Fadhil Mohammed, Ghanim Abdulkareem Mughir

Electrical Engineering Department, Faculty of Engineering, Mustansiriyah University, Baghdad, Iraq

## Article Info

### Article history:

Received Jul 21, 2021

Revised Apr 7, 2022

Accepted May 5, 2022

### Keywords:

Bit-error-rate

Exponential fading channel

Gamma fading channel

Orthogonal frequency division multiplexing

Signal-to-noise ratio

## ABSTRACT

Orthogonal frequency division multiplexing (OFDM) is a multicarrier modulation (MCM) technique that divides the wide bandwidth into parallel narrow bands, each of which is modulated by orthogonal subcarriers. Currently, OFDM is a high-spectral efficiency modulation technique that is used in a variety of wired and wireless applications. The transmitted signal in a wireless communication channel spreads from transmitter to receiver through multiple reflective paths. This triggers multipath fading, which causes variations in the received signal's amplitude and phase. Slow/fast and frequency-selective/frequency-nonselective are the main types of multipath fading channels. Therefore, in this paper, we proposed new models for modeling multipath fading channels, such as the exponential fading channel and the Gamma fading channel. In addition, new bit-error-rate (BER) derivations have been derived. The performance of the OFDM system over proposed channel models has been evaluated using Monte-Carlo simulation and compared to the Rayleigh fading channel model. The obtained results via simulations show that the exponential fading channel at a rate parameter ( $\lambda=0.5$ ) outperforms the Rayleigh fading channel by 6 dB for all values of  $E_b/N_0$ , while the Gamma fading channel at ( $\alpha=2$ ) outperforms the Rayleigh fading channel by 3 dB for all values of  $E_b/N_0$ .

This is an open access article under the [CC BY-SA](https://creativecommons.org/licenses/by-sa/4.0/) license.



## Corresponding Author:

Hasan Fadhil Mohammed

Department of Electrical Engineering, Faculty of Engineering, Mustansiriyah University

Baghdad, Iraq

Email: eema1032@uomustansiriyah.edu.iq

## 1. INTRODUCTION

The growing interest in wireless broadband communications and interactive media has fueled intense study on data rate transmission, bandwidth efficiency, and bit-error-rate (BER) performance across multipath fading channels [1]. Since the information to be sent is modulated into a single carrier in a conventional communication system, a single fade or interferer may cause the whole connection to fail. To achieve high bit rates, the symbols must be sent rapidly, using the full bandwidth. When a channel is frequency selective, its impulse response may span several symbol periods, resulting in what is referred to as intersymbol interference (ISI). This is a significant issue in wideband transmission across multipath fading channels, since it makes it more difficult to identify the sent signal, thus degrading the system's performance significantly [2]. Orthogonal frequency division multiplexing (OFDM) has been explored for a variety of wireless (applications, standards) and wired because of its popular features of high bandwidth efficiency, easy channel equalization, and immunity to multipath fading channels [3], [4]. This modulation method may be utilized effectively and consistently for high-speed digital data transmission across multipath fading

channels, since it splits the available bandwidth into multiple orthogonal data streams [5]. As a result, fading will impact a very small proportion of the subcarriers. Each subchannel will occupy a small frequency interval in the frequency domain, where the channel frequency response will be almost constant and each symbol will experience a nearly flat fading channel. Therefore, it is seen as one of the most promising solutions to the ISI problem [2]. Intercarrier interference (ICI) is eliminated when orthogonal subcarriers are used, and the signals carried on the various subcarriers do not interfere [6]. Hence, a simple frequency domain equalization method can be used [7]. IEEE 802.11 a, g, and n, IEEE 802.16a, and terrestrial digital video broadcasting (DVB-T) have all adapted it [8] and OFDM is used in digital subscriber line (DSL) and asymmetrical digital subscriber line (ADSL) for wired applications [9]. In the last few years, there have been a lot of studies done on the success of wireless channel models. In [10], the study of the performance evaluation of the OFDM-based 256 and 1024-QAM under multipath fading propagation circumstances defines the acceptable signal-to-noise ratio (SNR). In [11], focuses on the performance evaluation and investigation of OFDM systems operating across multipath fading channels like additive white Gaussian noise (AWGN), Rician, and Rayleigh. In [12] OFDM is studied and simulated in the presence of Rayleigh fading channels using channel estimation and equalization. Bit error probability is used to quantify performance. In [13], it analyzes the bit error rate (BER) performance of discrete cosine transform (DCT)-based OFDM and compares it to discrete fourier transform (DFT)-based OFDM to determine which modulation scheme performs better. In [14] The cyclic prefix's effect on the OFDM system's performance was investigated. The BER for different lengths of the cyclic prefix was compared using an OFDM transceiver equipped with a 16-QAM modulation method, highlighting the effect of channel noise.

In this paper we suggested new models to find new simulations and effects as well as to improve the BER performance of the OFDM system. In addition, two fading channel scenarios: exponential fading channel and Gamma fading channel have been adopted in this paper. The major contributions to this paper are related to improving the signal detection and enhancing the BER performance analysis of 4-QAM/OFDM over Gamma fading channels and exponential fading channels in AWGN based on the following: i) we derive the real part, the imaginary part of the channel impulse response in the time domain, in addition to the effective probability distribution and the effective SNR distribution of the Exponential and Gamma fading channels in the frequency domain at the OFDM demodulator output by using the central limit theorem (CLT), ii) we derive the variance in each dimension, i.e., the real part and the imaginary part of the exponential and Gamma fading channels, iii) we derive the BER based on the effective derived SNR distribution in the Gaussian noise only and in the presence of the exponential and Gamma fading channels in AWGN, and iv) we detect the received signal by using an optimum detector based on the Euclidean distance depending on the derived effective probability distribution at the OFDM demodulator output.

The rest of this paper is organized as follows: section 2 system model, while section 3 is the derivation of the variance in the time domain for exponential distribution and Gamma distribution. Section 4 BER performance analysis of M-ARY digital modulation over AWGN, exponential and Gamma fading channels, section 5 describes the simulation results and section 6 concludes this paper.

## 2. RESEARCH METHOD

### 2.1. System model

In this paper, the binary data bits  $d_k$  are divided into two-bit classes before being converted into the  $2^2$  symbols of a 4-QAM constellation to obtain the modulated symbols  $X=M(c)$  according to constellation mapping  $c$  shown in Figure 1 [15]. The complex base-band OFDM signal  $x_n$  can then be obtained in the time domain using an  $N$ -points inverse fast fourier transform (IFFT), as seen in [16].

$$x_n = \frac{1}{\sqrt{N}} \sum_{i=0}^{N-1} X_i e^{j\frac{2\pi ni}{N}}, \quad 0 \leq n \leq N-1 \quad (1)$$

where  $X_i$  the complex modulated symbol and  $N$  is the number of orthogonal subcarriers.

To minimize ISI between consecutive OFDM symbols in multipath fading channels, a time-domain CP of duration  $N_{CP}$  samples is added at the beginning of each OFDM symbol to produce the transmitted symbol  $\hat{x} = [x_N - N_{CP}, x_N - N_{CP} + 1, \dots, x_N - 1, x_0, x_1, x_N - 1]$ , which is programmed to exceed the cumulative delay spread of the fading channel. Then,  $\hat{x}$  is transmitted through the fading channel [17]. This signal is combined with additive noise in the wireless channel, resulting in the obtained signal as shown in (2) [18]:

$$y = h \otimes \hat{x} + w \quad (2)$$

where  $\otimes$  represents the convolution operation,  $h$  represents the complex impulse response coefficients in the time domain of the multipath fading channel and  $w$  is the AWGN.

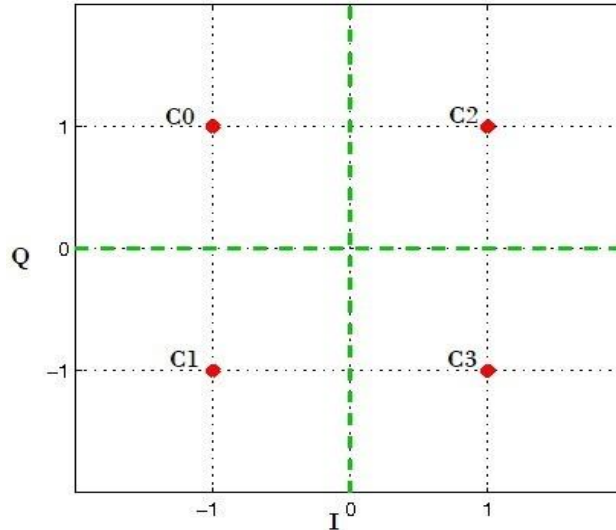


Figure 1. The four signal points of 4-QAM modulation in the constellation diagram

The multipath fading channel of wireless communication was modeled using exponential distribution or Gamma distribution in [19], [20] due to the fact that a large number of distributions used to model the multipath fading and shadowing fading channels for survival analysis are special instances of the generalized gamma distribution, such as the exponential and the gamma distributions [19], [21], as explained in more detail in this section. If the amplitude of the complex random variables  $h$  of the channel impulse response follows the exponential distribution in the time domain, the distribution can be expressed in [20] as in (3):

$$f_h(h) = \lambda e^{-\lambda h}, 0 \leq h < \infty, \lambda > 0 \tag{3}$$

where  $\lambda$  is the rate parameter of the fading channel.

The main concern with the fading can be stated into real and imaginary parts expressed as  $h_r$  and  $h_i$ , respectively. Assuming the magnitude of the fading channel  $h$  in the time domain,  $|h| = \sqrt{h_r^2 + h_i^2}$ , exhibits an exponential distribution where  $h = h_r + jh_i$ . Two random parameters are expanded by  $\theta$ , which is a randomly distributed random variable between the limits of the bounds  $\pi$  and  $-\pi$ , creating two further random variables as in (4) and (5).

$$h_r = |h| \cos(\theta) \tag{4}$$

$$h_i = |h| \sin(\theta) \tag{5}$$

As a result, the PDF of the real part of the multipath fading channel can be expressed as (6) [22].

$$\frac{dh_r}{dh} = \cos(\theta) \tag{6}$$

Then,  $f(h_r)|\theta$  a conditional PDF of  $h_r$  subjected to  $\theta$ , can be written as (7) [22].

$$\begin{aligned} f(h_r)|\theta &= \frac{f(h)}{dh_r/dh} = \lambda e^{-\lambda h} \frac{1}{dh_r/dh} \\ &= \frac{\lambda}{|\cos(\theta)|} e^{\frac{-\lambda h}{\cos(\theta)}} \end{aligned} \tag{7}$$

Moreover,  $f(h_i)|\theta$  a conditional PDF of  $h_i$  subjected to  $\theta$ , can be written as (8):

$$\begin{aligned} f(h_i)|\theta &= \frac{f(h)}{dh_i/dh} = \lambda e^{-\lambda h} \frac{1}{dh_i/dh} \\ &= \frac{\lambda}{|\sin(\theta)|} e^{\frac{-\lambda h}{\sin(\theta)}} \end{aligned} \tag{8}$$

Then the complex received signal,  $y$ , processed using the CP removal and fast Fourier transform (FFT) operation [18]. As a result, in the frequency domain, the complex signal can be represented as (9):

$$\begin{aligned} Y &= HX + W \\ Y_r + jY_i &= (H_r + jH_i)(X_r + jX_i) + (W_r + jW_i) \end{aligned} \quad (9)$$

where  $Y$ ,  $H$ ,  $X$ , and  $W$  represent the complex received signal in the frequency domain, the transfer function of the complex fading channel, complex modulated signals in the frequency domain, and AWGN, respectively.

Hence, the distribution of the real part,  $f(H_r)$  and the imaginary part,  $f(H_i)$  would approach a Gaussian distribution after the FFT operation with a mean equal to zero,  $\mu=0$ , and variance  $\sigma_{h_r}^2$  and  $\sigma_{h_i}^2$  computed in the next section. According to the central limit theorem (CLT) [23] as (10).

$$f(H_r) = \frac{1}{\sqrt{2\pi\sigma_{h_r}^2}} e^{-\frac{H_r^2}{2\sigma_{h_r}^2}} \quad (10)$$

$$f(H_i) = \frac{1}{\sqrt{2\pi\sigma_{h_i}^2}} e^{-\frac{H_i^2}{2\sigma_{h_i}^2}} \quad (11)$$

As a result, the magnitude of the fading channel in the frequency domain can be computed as  $|H| = \sqrt{H_r^2 + H_i^2}$  would follow the Rayleigh distribution with variance  $\sigma_h^2$  computed in the next section as (12):

$$f(H) = \frac{|H|}{\sigma_h^2} e^{-\frac{|H|^2}{2\sigma_h^2}} \quad (12)$$

with uniformly phase distributed in the range  $[-\pi, \pi)$ . Moreover, if the amplitude of the complex random variables  $h$ ,  $|h| = \sqrt{h_r^2 + h_i^2}$  of the channel impulse response follows the Gamma distribution in the time domain, the PDF can be expressed in [20] as (13):

$$f_h(h) = \frac{1}{\Gamma(\alpha)\beta^\alpha} h^{\alpha-1} e^{-\frac{h}{\beta}}, 0 < h < \infty, \alpha > 0, \beta > 0 \quad (13)$$

where  $\alpha$  is the shape parameter and  $\beta$  is the scale parameter. Following the same mentioned discussions, the distribution of  $f(h_r)|\theta$  and  $f(h_i)|\theta$  can be derived as (14) and (15).

$$\begin{aligned} f(h_r)|\theta &= \frac{f(h)}{dh_r/dh} = \frac{1}{\Gamma(\alpha)\beta^\alpha} h^{\alpha-1} e^{-\frac{h}{\beta}} \frac{1}{dh_r/dh} \\ &= \frac{1}{\Gamma(\alpha)\beta^\alpha |\cos(\theta)|} \left(\frac{h}{\cos(\theta)}\right)^{\alpha-1} e^{-\frac{h}{\beta \cos(\theta)}} \end{aligned} \quad (14)$$

and

$$\begin{aligned} f(h_i)|\theta &= \frac{f(h)}{dh_i/dh} = \frac{1}{\Gamma(\alpha)\beta^\alpha} h^{\alpha-1} e^{-\frac{h}{\beta}} \frac{1}{dh_i/dh} \\ &= \frac{1}{\Gamma(\alpha)\beta^\alpha |\sin(\theta)|} \left(\frac{h}{\sin(\theta)}\right)^{\alpha-1} e^{-\frac{h}{\beta \sin(\theta)}} \end{aligned} \quad (15)$$

Thanks to the central limit theorem after FFT operation, which makes the distribution of the real and imaginary components of the Gamma fading channel approaches Gaussian distribution as expressed in (10) and (11) in the next section with  $\mu=0$  and variance  $\sigma_{h_r}^2$  and  $\sigma_{h_i}^2$  computed in the next section. Therefore, the magnitude of the fading channel with Gamma distribution will follow Rayleigh distribution as given in (12) and the phase will follow uniform distribution throughout the frequency domain from the range  $[-\pi, \pi)$ . Finally, the received signal in (9) can be detected using maximum likelihood (ML) detection. The ML can be implemented by finding the minimum Euclidean distance between all the possible transmitted symbols over the channel  $H$  and the received signal  $Y$  as [24]:

$$\widehat{d}_k = \arg \min_{X \in C} \|Y - H.X\|^2 \tag{16}$$

where C=C1, C2, C3, C4 represents a collection of all possible symbols X in a 4-QAM constellation as presented in Figure 1.

The bit error rate (BER) is determined by comparing the binary data bits generated by the source at the transmitter,  $d_k$ , with the eventually obtained bits at the receiver,  $\widehat{d}_k$ , and then dividing the result by the number length of  $d_k$  [25]. Figure 2 illustrates the configuration of an OFDM transceiver system (transmitter and receiver) [26], [27].

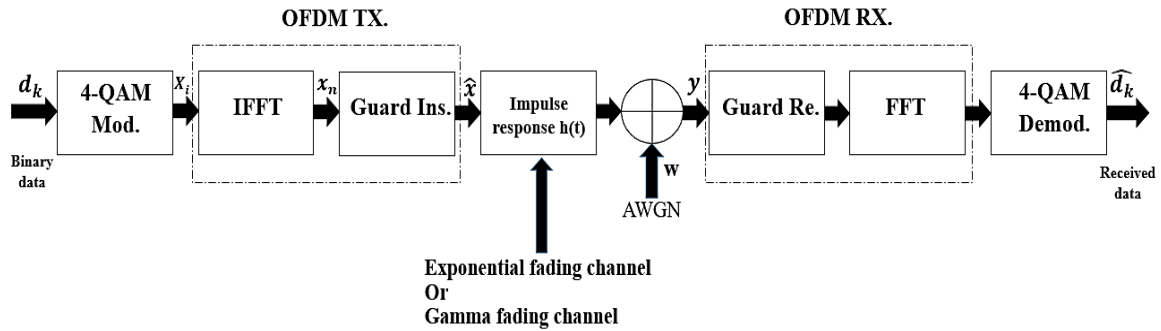


Figure 2. Baseband OFDM system model over exponential/Gamma fading channel

## 2.2. Derivation of the variance in the time domain for exponential distribution and gamma distribution

### 2.2.1. Variance derivation of exponential distribution

Suppose the magnitude of the complex random variable  $h$  in the time domain follows the exponential distribution, that is, it has pdf given by (3). Hence, the variance can be computed as in (17) [20]:

$$\sigma_h^2 = E(|h|^2) - |E(h)|^2 \tag{17}$$

where  $E(|h|^2)$  is the second moment and  $|E(h)|^2$  is the square of the first moment (expected value).

The variance of an exponential distribution is computed in [20] as  $\sigma_h^2 = \frac{1}{\lambda^2}$ . However, the mean and variance of a complex random variable,  $h = h_r + jh_i$ , can be expressed as given in [24] as  $E(h) = E(h_r) + jE(h_i)$  and  $\sigma_h^2 = \sigma_{h_r}^2 + \sigma_{h_i}^2$ . So, the variance of the real component  $\sigma_{h_r}^2$ , is equal to the variance of the imaginary component  $\sigma_{h_i}^2$  and the variance in each dimension is:

$$\sigma_{h_r}^2 = \sigma_{h_i}^2 = \frac{\sigma_h^2}{2} = \frac{1}{2\lambda^2} \tag{18}$$

### 2.2.2. Variance derivation of gamma distribution

If the magnitude of the complex random variable  $h$  follows the Gamma distribution as given in (13), the variance can be expressed as given in [28] as  $\sigma_h^2 = \alpha\beta^2$ , hence, the variance in each dimension can be expressed as mentioned above as (19).

$$\sigma_{h_r}^2 = \sigma_{h_i}^2 = \frac{\sigma_h^2}{2} = \frac{\alpha\beta^2}{2} \tag{19}$$

## 2.3. BER performance analysis of QAM over AWGN, exponential and gamma fading channels

The influence of fading is measured using 4-QAM modulation. The bit error rate (BER), is a more accurate performance parameter for measuring modulation schemes. In a slow flat fading path, the following integral may be used to measure the BER performance of any digital modulation scheme [29].

$$P_b = \int_0^\infty P_{b,AWGN}(\gamma)P_{df}(\gamma) d\gamma \tag{20}$$

The error probability of a specific modulation scheme in an AWGN channel at a specified signal-to-noise ratio is:

$$\gamma = h^2 \frac{E_b}{N_o} \quad (21)$$

where  $h$  is the random variable of channel gain, in a non-fading AWGN channel,  $\frac{E_b}{N_o}$  is the ratio of the bit energy to the noise power density. The random variable  $h^2$  denotes the fading channel's instantaneous power and  $P_{df}(\gamma)$  is the probability density function of  $\gamma$  due to the fading channel [29].

### 2.3.1. Derivation of BER of 4-QAM digital modulation in AWGN channel

The cumulative distribution function (CDF) of a continuous random variable  $X$  can be expressed as the integral of its probability density function  $p_X$  follows [20]:

$$F_X(x) = \int_{-\infty}^x p_X(t) dt \quad (22)$$

The probability of error receiving the constellation symbol  $C_2=1+1j$  over AWGN channels as shown in Figure 1 can be computed as (23) [30].

$$P_e(C_2) = F_X^{C_2}(0) + F_Y^{C_2}(0) - F_X^{C_2}(0)F_Y^{C_2}(0) \quad (23)$$

Because of the symmetry, the marginal probabilities for the real and imaginary components can be calculated using the Gaussian PDF as (24).

$$F_X^{C_2}(0) = F_Y^{C_2}(0) \quad (24)$$

The equation of Gaussian PDF is:

$$p(x) = \frac{1}{\sqrt{2\pi\sigma^2}} e^{-\frac{(x-\mu)^2}{2\sigma^2}}, \text{ with } \mu = 0 \text{ and } \sigma^2 = \frac{N_o}{2} \quad (25)$$

So

$$F_X^{C_2}(0) = \int_{-\infty}^0 \frac{1}{\sqrt{2\pi\sigma_w^2}} e^{-\frac{(x-\sqrt{\frac{E_s}{2}})^2}{2\sigma_w^2}} dx = \frac{1}{2} \operatorname{erf}\left(-\sqrt{\frac{E_s}{4\sigma_w^2}}\right) - \frac{1}{2} \operatorname{erf}(-\infty)$$

$$F_X^{C_2}(0) = \frac{1}{2} - \frac{1}{2} \operatorname{erf}\left(\sqrt{\frac{\gamma}{2}}\right), \text{ where } \gamma = \frac{E_s}{2\sigma_w^2} \quad (26)$$

As shown in (26) can be rewritten as (27):

$$F_X^{C_2}(0) = \frac{1}{2} \operatorname{erfc}\left(\sqrt{\frac{\gamma}{2}}\right) \quad (27)$$

Now we substitute (27) into (23) we get:

$$P_e(C_2) = \frac{1}{2} \operatorname{erfc}\left(\sqrt{\frac{\gamma}{2}}\right) + \frac{1}{2} \operatorname{erfc}\left(\sqrt{\frac{\gamma}{2}}\right) - \frac{1}{2} \operatorname{erfc}\left(\sqrt{\frac{\gamma}{2}}\right) \frac{1}{2} \operatorname{erfc}\left(\sqrt{\frac{\gamma}{2}}\right)$$

$$= \operatorname{erfc}\left(\sqrt{\frac{\gamma}{2}}\right) - \frac{1}{4} \operatorname{erfc}^2\left(\sqrt{\frac{\gamma}{2}}\right)$$

$$\approx \operatorname{erfc}\left(\sqrt{\frac{\gamma}{2}}\right) \text{ for } \gamma \gg 0 \quad (28)$$

Due to the constellation symmetry in Figure 1, the error probability of  $C_2$  is equal to the error probability of  $C_0$ ,  $C_1$  and  $C_3$ . The total symbol error probability can be expressed as (29).

$$P_s(C) = P(C_0) P_e(C_0) + P(C_1) P_e(C_1) + P(C_2) P_e(C_2) + P(C_3) P_e(C_3) \quad (29)$$

We assume that four symbols are transmitted with equal probability, so  $P(C_0) = P(C_1) = P(C_2) = P(C_3) = \frac{1}{4}$ , hence, the net symbol error probability can be expressed as (30).

$$\begin{aligned} P_s(C) &= \frac{1}{4} (P_e(C0) + P_e(C1) + P_e(C2) + P_e(C3)) = \frac{1}{4} \left( 4 \operatorname{erfc} \left( \sqrt{\frac{\gamma}{2}} \right) \right) \\ &= \operatorname{erfc} \left( \sqrt{\frac{\gamma}{2}} \right) \end{aligned} \quad (30)$$

Therefore, the BER of the 4-QAM constellation can be computed as (31):

$$\begin{aligned} P_b(C) &= \frac{P_s(C)}{\log_2 M} = \frac{P_s(C)}{2} \\ P_b(C) &= \frac{1}{2} \operatorname{erfc} \left( \sqrt{\frac{E_b}{2\sigma_w^2}} \right) \end{aligned} \quad (31)$$

Leads to the

$$\operatorname{BER}_{4\text{QAM,AWGN}} = \frac{1}{2} \operatorname{erfc} \left( \sqrt{\frac{E_b}{N_o}} \right) \quad (32)$$

### 2.3.2. Derivation of BER of 4-QAM digital modulation in exponential fading channel

For the exponential fading channel as expressed in (3) in the time domain, the H follows the Rayleigh distribution in the frequency domain after FFT operation based on CLT as computed in (12), and  $|H|^2$  has a chi-square distribution of two degrees of freedom as expressed in (33) [29]:

$$P_{df}(\gamma) = \frac{1}{\bar{\gamma}} \exp \left( -\frac{\gamma}{\bar{\gamma}} \right) \quad (33)$$

where  $\bar{\gamma} = \frac{E_b}{N_o} E[|H|^2]$  is the signal-to-noise ratio on average for  $E[|H|^2] = 1/\lambda^2$ , substituting in (33), gets

$$P_{df}(\gamma) = \frac{1}{(1/\lambda^2)E_b/N_o} e^{-\frac{\gamma}{(1/\lambda^2)E_b/N_o}} \quad (34)$$

Substituting (32) and e (34) in (20) we get:

$$\begin{aligned} P_b &= \int_0^\infty \frac{1}{2} \operatorname{erfc}(\sqrt{\gamma}) * \frac{1}{(1/\lambda^2)E_b/N_o} e^{-\frac{\gamma}{(1/\lambda^2)E_b/N_o}} d\gamma \\ &= \left( -\frac{(1/\lambda)\sqrt{E_b/N_o} \operatorname{erf} \left( \frac{\sqrt{\gamma(1/\lambda^2)(E_b/N_o)+1}}{(1/\lambda)\sqrt{E_b/N_o}} \right)}{2\sqrt{(1/\lambda^2)(E_b/N_o)+1}} - \frac{1}{2} \operatorname{erfc}(\sqrt{\gamma}) e^{-\frac{\gamma}{(1/\lambda^2)E_b/N_o}} \right) \Bigg|_0^\infty \end{aligned}$$

The equation after substituting the integral values becomes:

$$\begin{aligned} &= \left[ -\frac{\left(\frac{1}{\lambda}\right)\sqrt{E_b/N_o} \operatorname{erf}(\infty)}{2\sqrt{\left(\frac{1}{\lambda^2}\right)(E_b/N_o)+1}} - \frac{1}{2} \operatorname{erfc}(\infty) e^{-\frac{\infty}{\left(\frac{1}{\lambda^2}\right)E_b/N_o}} \right] - \left[ -\frac{(1/\lambda)\sqrt{E_b/N_o} \operatorname{erf}(0)}{2\sqrt{(1/\lambda^2)(E_b/N_o)+1}} - \frac{1}{2} \operatorname{erfc}(0) e^{-\frac{0}{\left(\frac{1}{\lambda^2}\right)E_b/N_o}} \right] \\ &\text{where } \operatorname{erf}(\infty) = 1, \operatorname{erfc}(\infty) = 0, \operatorname{erf}(0) = 0, \operatorname{erfc}(0) = 1 \\ &= -\frac{(1/\lambda)\sqrt{E_b/N_o}}{2\sqrt{(1/\lambda^2)(E_b/N_o)+1}} + \frac{1}{2} \end{aligned} \quad (35)$$

As shown in (35) can be rewritten as (36).

$$P_b = \frac{1}{2} \left( 1 - \frac{\sqrt{1/\lambda^2 E_b/N_o}}{\sqrt{1/\lambda^2 (E_b/N_o) + 1}} \right) \quad (36)$$

### 2.3.3. Derivation of BER of 4-QAM digital modulation in gamma fading channel

Using the same steps that are used to find the  $P_{df}(\gamma)$  of the exponential fading channel, the  $P_{df}(\gamma)$  for the Gamma fading channel is:

$$P_{df}(\gamma) = \frac{1}{\alpha\beta^2 E_b/N_0} e^{-\frac{\gamma}{\alpha\beta^2 E_b/N_0}} \quad (37)$$

Sub (32) and (37) in (20) we get:

$$P_b = \int_0^\infty \frac{1}{2} \operatorname{erfc}(\sqrt{\gamma}) * \frac{1}{\alpha\beta^2 E_b/N_0} e^{-\frac{\gamma}{\alpha\beta^2 E_b/N_0}} d\gamma$$

$$= \left( -\frac{\frac{\sqrt{\alpha\beta^2 * E_b/N_0} \operatorname{erf}\left(\frac{\sqrt{\gamma(\alpha\beta^2(E_b/N_0)+1)}}{\sqrt{\alpha\beta^2 * E_b/N_0}}\right)}{2\sqrt{\alpha\beta^2(E_b/N_0)+1}} - \frac{1}{2} \operatorname{erfc}(\sqrt{\gamma}) e^{-\frac{\gamma}{\alpha\beta^2 * (E_b/N_0)}}}{0} \right)_0^\infty$$

The equation after substituting the integral values becomes:

$$= \left[ -\frac{\sqrt{\alpha\beta^2 * E_b/N_0} \operatorname{erf}(\infty)}{2\sqrt{\alpha\beta^2(E_b/N_0)+1}} - \frac{1}{2} \operatorname{erfc}(\sqrt{\infty}) e^{-\frac{\infty}{\alpha\beta^2 * (E_b/N_0)}} \right] - \left[ -\frac{\sqrt{\alpha\beta^2 * E_b/N_0} \operatorname{erf}(0)}{2\sqrt{\alpha\beta^2(E_b/N_0)+1}} - \frac{1}{2} \operatorname{erfc}(\sqrt{0}) e^{-\frac{0}{\alpha\beta^2 * (E_b/N_0)}} \right]$$

$$= -\frac{\sqrt{\alpha\beta^2 * E_b/N_0}}{2\sqrt{(\alpha\beta^2 * E_b/N_0)+1}} + \frac{1}{2} \quad (38)$$

As shown in (38) can be rewritten as (39).

$$P_b = \frac{1}{2} \left( 1 - \frac{\sqrt{\alpha\beta^2 * E_b/N_0}}{\sqrt{(\alpha\beta^2 * E_b/N_0)+1}} \right) \quad (39)$$

### 3. SIMULATION RESULTS AND DISCUSSION

The BER performances are investigated using the MATLAB simulation program for 4-QAM/OFDM over two different channel distributions such as the multipath exponential fading channel and the multipath Gamma fading channel in AWGN, and the results are compared with the 4-QAM/OFDM over the Rayleigh fading channel. The following simulation parameters were set, the number of sub-carriers was set as N=64 and CP=16, the constellation size was set as 4-QAM and the system bandwidth was set at 20 MHz for the ITU pedestrian standard channel for multipath exponential fading channel and multipath Gamma fading channel are used, as shown in Table 1 [31].

Table 1. ITU channel profile

ITU Pedestrian Ch.103		
Path n	Power (dB)	Delay (μs)
1	0	0
2	-0.9	0.2
3	-4.9	0.8
4	-8	1.2
5	-7.8	2.3
6	-23.9	3.7

#### 3.1. Performance of 4-QAM/OFDM system over exponential fading channel

We are interested in this section to show the matching of the derived distributions with simulated results in the time domain based on (3) and the frequency domain based on e (12), for  $\sigma_h^2$  computed in (18). In Figure 3, we see the exponential fading histograms, where the parameters are set to  $\lambda=0.5$ ,  $\lambda=1$  and  $\lambda=1.5$ , respectively. It should be noted that (3) and the derived closed-form PDF in (12) have similar analytical distributions to those of the simulation results in the probability domain.

The impact of changing  $\lambda$  parameter on the BER performance of the 4-QAM/OFDM system over exponential fading channels and AWGN compared to the Rayleigh fading channel is shown in Figure 4. Simulations were run over different scenarios of the channel effect by changing the scale parameter  $\lambda$  to 0.5, 1, and 1.5 for severe impact, normal impact, and low impact, respectively. For instance, in the case of the

normal impact, the exponential fading channel has the same effect as the Rayleigh fading channel, and in this case, the parameter of  $\lambda$  is chosen as follows:

The PDF of the signal to noise ratio distribution at the OFDM demodulator output can be derived based on CLT as given in (34), while in the Rayleigh fading channel it can be expressed as in [32].

$$P_{df}(\gamma) = \frac{1}{(2\sigma^2)E_b/N_o} e^{\frac{-\gamma}{(2\sigma^2)E_b/N_o}} \tag{40}$$

Hence, both distributions have the same effect when

$$\frac{1}{\lambda^2} = 2\sigma^2$$

By take the square root for both sides:

$$\frac{1}{\lambda} = \sqrt{2}\sigma$$

The standard deviation  $\sigma = \frac{1}{\sqrt{2}}$  in both directions of the Rayleigh distribution. Hence,

$$\frac{1}{\lambda} = \sqrt{2} \frac{1}{\sqrt{2}} \text{ so } \lambda = 1$$

Based on the first value ( $\lambda = 0.5$ ), we determined that the BER performance of the 4-QAM/OFDM method over an exponential fading channel is superior to that of the system over a Rayleigh fading channel. At the second value ( $\lambda = 1$ ), the BER performance of the exponential fading channel is close to or similar to that of the Rayleigh fading channel. But on the third value ( $\lambda = 1.5$ ) the performance will be worse. Table 2 shows the BER performance of the proposed system compared to the conventional system at  $E_b/N_o = 20$  dB. The Table 2 shows that the BER improved by decreasing the rate parameter  $\lambda$ , and the performance is matched to the conventional system over Rayleigh fading channel when  $\lambda = 1$ .

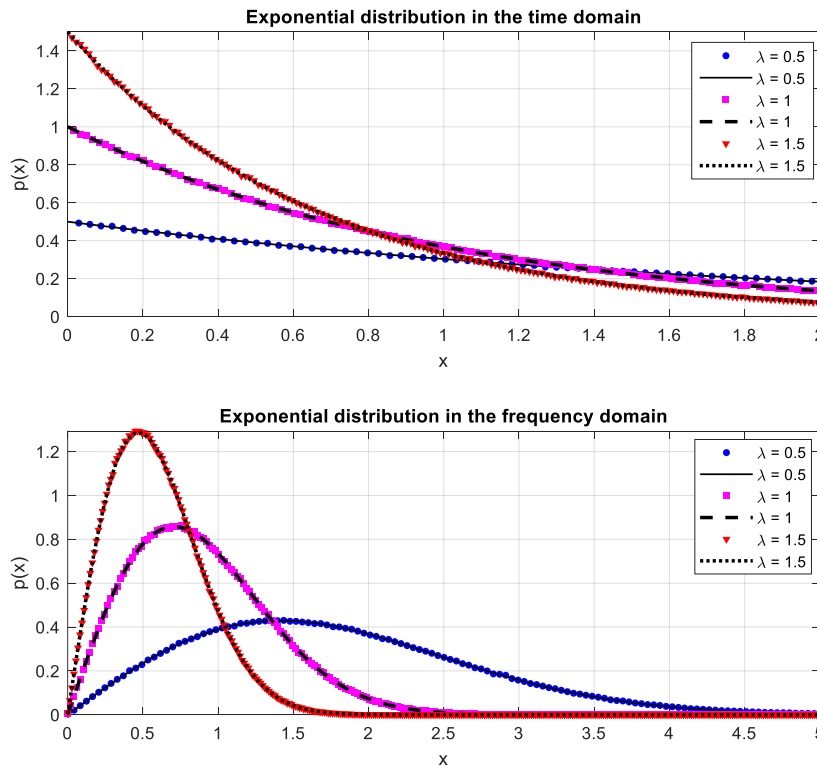


Figure 3. Simulated Vs histogram plots in the time domain and the frequency domain for exponential fading channel

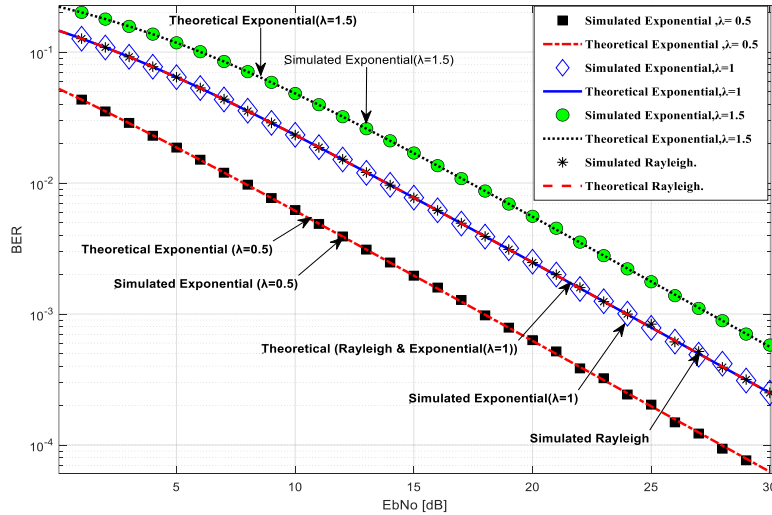


Figure 4. Performance of 4-QAM/OFDM system over exponential fading channel

Table 2. BER values with different scenarios of  $\lambda$  parameter

$\lambda$ parameter	BER (Exponential)	BER (Rayleigh)
0.5	$0.6238 \times 10^{-3}$	$0.2481 \times 10^{-2}$
1	$0.2481 \times 10^{-2}$	$0.2481 \times 10^{-2}$
1.5	$0.5532 \times 10^{-2}$	$0.2481 \times 10^{-2}$

### 3.2. Performance of 4-QAM/OFDM system over gamma fading channel

A comparison of the histogram plots of the derived distributions with simulated results for Gamma distribution as presented in the time domain in (13) and in the frequency domain will follow the Rayleigh distribution as given in (12), for  $\sigma_h^2$  computed in (19). In Figure 5, we see the Gamma fading histograms, where the parameters are set to  $\alpha=0.5$ ,  $\alpha=1$  and  $\alpha=2$  for  $\beta=1$ . It should be noted that (13) and the derived closed-form PDF in (12) have similar analytical distributions to those of the simulation results in the probability domain.

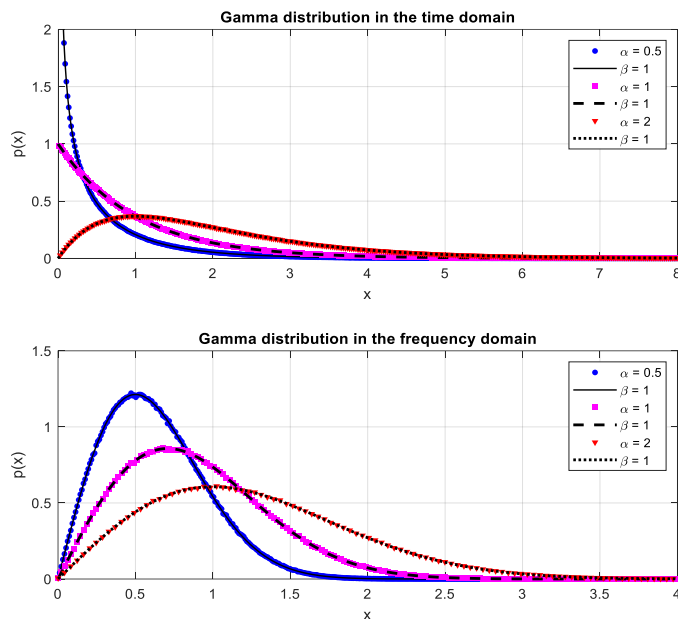


Figure 5. Simulated Vs histogram plots in the time domain and the frequency domain for Gamma fading channel

The impact of changing  $\alpha$  and  $\beta$  parameters on the BER performance of 4-QAM/OFDM systems over Gamma fading channel and AWGN compared to Rayleigh fading channel is shown in Figure 6. Simulations were run for various values of the channel effect by changing the  $\alpha$  parameter (0.5, 1, 2) for severe impact, normal impact and low impact, respectively, and for the  $\beta$  parameter equal to 1, by using the same method to find the normal effect in the exponential fading channel, we found the normal effect in the Gamma fading channel at  $\alpha=1$ .

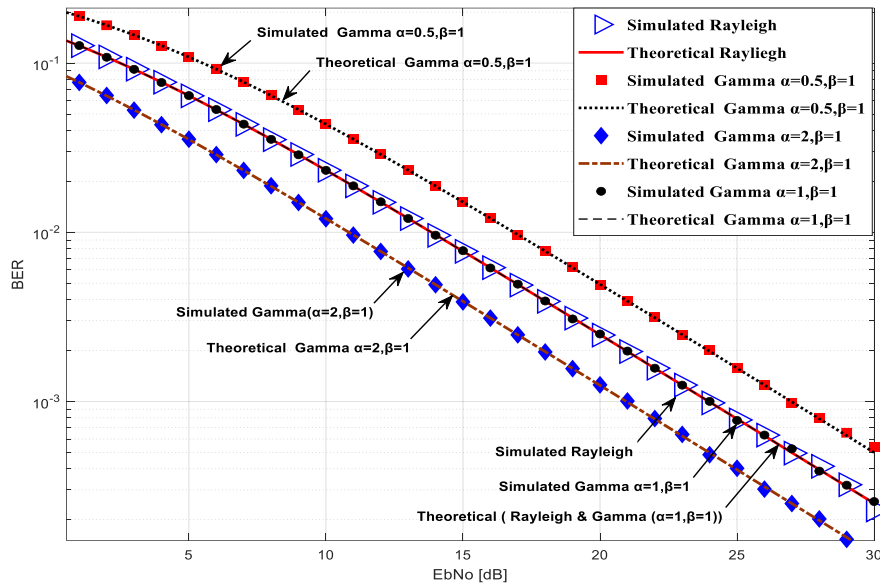


Figure 6. Performance of 4-QAM/OFDM system over gamma fading channel

In this figure, the BER performance of the 4-QAM/OFDM system over a Gamma fading channel is lower than that of the system over a Rayleigh fading channel based on the first value ( $\alpha=0.5$ ). Moreover, the BER performance of the Gamma fading channel is equal to or equivalent to that of the Rayleigh fading channel at the second value ( $\alpha=1$ ). Furthermore, the result will be better on the third value ( $\alpha=2$ ). Table 3 shows the BER performance of the proposed system compared to the conventional system at  $E_b/N_0=20$  dB. The Table 3 shows that the BER improved by increasing the shape parameter  $\alpha$ , and the performance is matched to the conventional system over Rayleigh fading channel when  $\alpha=1$ .

Table 3. BER values with different scenarios of Shape parameter ( $\alpha$ ) at  $\beta=1$

$\alpha$ parameter	BER (Gamma)	BER (Rayleigh)
0.5	$0.4899 \times 10^{-2}$	$0.2481 \times 10^{-2}$
1	$0.2481 \times 10^{-2}$	$0.2481 \times 10^{-2}$
2	$0.1245 \times 10^{-2}$	$0.2481 \times 10^{-2}$

#### 4. CONCLUSION

The BER of the 4-QAM/OFDM system in AWGN over different channel scenarios, such as exponential and Gamma fading channels, in addition to the BER performance, has been investigated for both channels in this paper. The simulation results obtained via the MATLAB program have confirmed the feasibility of the exact derived PDFs at the OFDM demodulator output in the frequency domain based on CLT, leading to derived exact new theoretical BER equations matching to the Monte-Carlo simulation for both proposed channel distributions. The 4-QAM OFDM system in AWGN over exponential fading channel with different  $\lambda$  parameters (0.5, 1, and 1.5) has been simulated. It has been shown from the results that the exponential fading channel outperforms the Rayleigh fading channel when ( $\lambda < 1$ ) for all values of  $E_b/N_0$ . Additionally, the 4-QAM OFDM system in AWGN over Gamma fading channel with different values for  $\alpha$  (0.5, 1, and 2) and for  $\beta=1$  has been simulated. It has been shown from the results that the Gamma fading channel outperforms the Rayleigh fading channel when ( $\alpha > 1$ ) for all values of  $E_b/N_0$ .

## REFERENCES

- [1] H. A. Leftah and H. N. Alminshid, "Channel capacity and performance evaluation of precoded MIMO-OFDM system with large-size constellation," *International Journal of Electrical and Computer Engineering (IJECE)*, vol. 9, no. 6, pp. 5024–5030, Dec. 2019, doi: 10.11591/ijece.v9i6.pp5024-5030.
- [2] M. A. Saeed, B. M. Ali, and M. H. Habaebi, "Performance evaluation of OFDM schemes over multipath fading channels," in *9th Asia-Pacific Conference on Communications (IEEE Cat. No.03EX732)*, 2003, vol. 1, pp. 415–419, doi: 10.1109/APCC.2003.1274387.
- [3] H. A. Leftah and S. Boussakta, "Novel OFDM based on C-transform for improving multipath transmission," *IEEE Transactions on Signal Processing*, vol. 62, no. 23, pp. 6158–6170, Dec. 2014, doi: 10.1109/TSP.2014.2362097.
- [4] Z. Na, Y. Wang, M. Xiong, X. Liu, and J. Xia, "Modeling and throughput analysis of an ADO-OFDM based relay-assisted VLC system for 5G networks," *IEEE Access*, vol. 6, pp. 17586–17594, 2018, doi: 10.1109/ACCESS.2018.2817487.
- [5] I. Kalet, "The multitone channel," *IEEE Transactions on Communications*, vol. 37, no. 2, pp. 119–124, 1989, doi: 10.1109/26.20079.
- [6] R. D. J. Van Nee and R. Prasad, *OFDM for wireless multimedia communications*. -2568: Artech House, Inc.685 Canton St. Norwood, MA, 2000.
- [7] M. K. Abboud and B. M. Sabbar, "Performance evaluation of high mobility OFDM channel estimation techniques," *International Journal of Electrical and Computer Engineering (IJECE)*, vol. 10, no. 3, pp. 2562–2568, Jun. 2020, doi: 10.11591/ijece.v10i3.pp2562-2568.
- [8] A. Panajotovic, F. Riera-Palou, and G. Femenias, "Adaptive Uniform channel decomposition in MU-MIMO-OFDM: Application to IEEE 802.11ac," *IEEE Transactions on Wireless Communications*, vol. 14, no. 5, pp. 2896–2910, May 2015, doi: 10.1109/TWC.2015.2396513.
- [9] P. Manhas and M. K. Soni, "OFDM system performance evaluation under Different fading channels and channel coding using MATLAB Simulink," *Indonesian Journal of Electrical Engineering and Computer Science (IJECS)*, vol. 5, no. 2, pp. 260–266, Feb. 2017, doi: 10.11591/ijeecs.v5.i2.pp260-266.
- [10] T. Ota, M. Nakamura, and H. Otsuka, "Performance evaluation of OFDM-based 256- and 1024-QAM in multipath fading propagation conditions," in *2017 Ninth International Conference on Ubiquitous and Future Networks (ICUFN)*, Jul. 2017, pp. 554–556, doi: 10.1109/ICUFN.2017.7993849.
- [11] K. Mahender, T. A. Kumar, and K. S. Ramesh, "Performance study of OFDM over multipath fading channels for next wireless communications," *International Journal of Applied Engineering Research*, vol. 12, no. 20, pp. 10205–10210, 2017.
- [12] D. V. Bhimsing and A. C. Bhagali, "Performance of channel estimation and equalization in OFDM system," in *2017 IEEE International Conference on Power, Control, Signals and Instrumentation Engineering (ICPCSI)*, Sep. 2017, pp. 1003–1005, doi: 10.1109/ICPCSI.2017.8391861.
- [13] A. Farzamia, E. Moung, B. V. Malitam, and M. K. Haldar, "BER analysis for OFDM systems with various modulation techniques in Rayleigh fading channel," in *2018 10th International Conference on Computational Intelligence and Communication Networks (CICN)*, Aug. 2018, pp. 40–44, doi: 10.1109/CICN.2018.8864950.
- [14] S. Zanafi and N. Aknin, "Analysis of cyclic prefix length effect on ISI limitation in OFDM system over a Rayleigh-fading multipath," *International Journal of Electrical and Computer Engineering (IJECE)*, vol. 11, no. 4, pp. 3114–3122, Aug. 2021, doi: 10.11591/ijece.v11i4.pp3114-3122.
- [15] A. B. Carlson, *Communication systems: an introduction to signals and noise in electrical communication/A. Bruce Carlson*, McGraw-Hil. McGraw-Hill Education, 1986.
- [16] G. A. Al-Rubaye, C. C. Tsimenidis, and M. Johnston, "Low-density parity check coded orthogonal frequency division multiplexing for PLC in non-Gaussian noise using LLRs derived from effective noise probability density functions," *IET Communications*, vol. 11, no. 16, pp. 2425–2432, Nov. 2017, doi: 10.1049/iet-com.2017.0265.
- [17] G. A. Al-Rubaye, C. C. Tsimenidis, and M. Johnston, "Performance evaluation of T-COFDM under combined noise in PLC with log-normal channel gain using exact derived noise distributions," *IET Communications*, vol. 13, no. 6, pp. 766–775, Apr. 2019, doi: 10.1049/iet-com.2018.6185.
- [18] A. Farzamia, N. W. Hlaing, M. Mariappan, and M. K. Haldar, "BER comparison of OFDM with M-QAM Modulation scheme of AWGN and Rayleigh fading channels," in *2018 9th IEEE Control and System Graduate Research Colloquium (ICSGRC)*, Aug. 2018, pp. 54–58, doi: 10.1109/ICSGRC.2018.8657503.
- [19] A. Abdi and M. Kaveh, "On the utility of gamma PDF in modeling shadow fading (slow fading)," in *1999 IEEE 49th Vehicular Technology Conference (Cat. No.99CH36363)*, 1999, vol. 3, pp. 2308–2312, doi: 10.1109/VETEC.1999.778479.
- [20] J. Tabak, *Probability and statistics: The science of uncertainty*. W. H. Freeman, Amazon, 2014.
- [21] J. M. Box-Steffensmeier, J. M. Box-Steffensmeier, and B. S. Jones, *Event history modeling: A guide for social scientists*. Cambridge University Press, 2004.
- [22] S. U. Pillai and A. Papoulis, *Probability, random variables, and stochastic processes*, Fourth Edi. McGraw-Hill Companies, 2001.
- [23] A. Goldsmith, *Wireless communications*. Cambridge University Press, 2005.
- [24] J. G. Proakis and M. Salehi, *Digital communications*, 5th Editio. McGraw-Hill Companies, Inc., 2008.
- [25] G. A. AlKareem, "Three dimensional concatenated codes in OFDM transmission system under a Rayleigh fading channel with carrier li," *Journal of Engineering and Development*, vol. 12, no. 2, 2008.
- [26] T. Cui and C. Tellambura, "Joint data detection and channel estimation for OFDM systems," *IEEE Transactions on Communications*, vol. 54, no. 4, pp. 670–679, Apr. 2006, doi: 10.1109/TCOMM.2006.873075.
- [27] P. Sure and C. M. Bhumra, "A survey on OFDM channel estimation techniques based on denoising strategies," *Engineering Science and Technology, an International Journal*, vol. 20, no. 2, pp. 629–636, Apr. 2017, doi: 10.1016/j.jestch.2016.09.011.
- [28] R. L. B. G. Casella, *Statistical inference*, 2nd editio. Cengage Learning, 2002.
- [29] K. D. Rao, *Channel coding techniques for wireless communications*. New Delhi: Springer India, 2015.
- [30] G. A. Al-Rubaye, C. C. Tsimenidis, and M. Johnston, "Improved performance of TC-OFDM-PLNC for PLCs using exact derived impulsive noise PDFs," in *2017 IEEE International Conference on Communications Workshops (ICC Workshops)*, May 2017, pp. 1271–1276, doi: 10.1109/ICCW.2017.7962833.
- [31] I.-R. Recommendation, "Guidelines for evaluation of radio transmission technologies for imt-2000," *Rec. ITU-R M. 1225*. 1997.
- [32] K.-L. Du and M. N. S. Swamy, *Wireless communication systems*, vol. 7. Cambridge: Cambridge University Press, 2010.

**BIOGRAPHIES OF AUTHORS**

**Hasan Fadhil Mohammed**    was born in Diyala, Iraq, in 1985. He received the B.Sc. in Electronic Engineering from Faculty of Engineering of Diyala University, Iraq in 2008. Currently, he is a master student in Electronics and Communications Engineering Department, Mustansiriyah University, Baghdad, Iraq. His recent research is mitigation of performance degradation by different fading channels for convolutional coded QAM/OFDM system over gaussian noise. He can be contacted at email: [ema1032@uomustansiriyah.edu.iq](mailto:ema1032@uomustansiriyah.edu.iq).



**Ghanim Abdulkareem Mughir**    is a Lecturer in the Electrical Engineering Department, Faculty of Engineering, Mustansiriyah University, Baghdad, Iraq. He received his M.Sc. in Electronics and Communications from Al-Mustansiriya University, Baghdad, Iraq, in 1999. He received his PhD from the School of Electrical and Electronics Engineering, Newcastle University, Newcastle Upon Tyne, U.K, in 2017. His research focuses on wired/wireless communications on coded systems, OFDM systems, fading and power line communication channels, channel modelling and receiver design. He can be contacted at email: [g.a.m.al-rubaye@uomustansiriyah.edu.iq](mailto:g.a.m.al-rubaye@uomustansiriyah.edu.iq).